

RESEARCH

Open Access



Changes in microbial and metabolic profiles of mice fed with long-term high salt diet

Huiying Tian^{1†}, Xiaotang Gao^{2†}, Hanlin Du², Zhuofeng Lin^{2*} and Xianen Huang^{3,4*}

Abstract

Purpose High salt diet (HSD) has been considered as a risk factor for the development of metabolic disorders. However, less is known about long-term implications of HSD. Therefore, the aim of this study was to conduct a preliminary investigation into the effects of mice feeding with long-term HSD on gut microbial and metabolic profiles.

Methods In this study, C57BL/6 J mice were fed with HSD for 22 weeks, after which fat and feces were collected. The composition of fecal microbiota was determined using 16S rRNA gene sequencing. Fecal metabolic profiling of mice was identified through untargeted ultrahigh-performance liquid chromatography-mass spectrometry. In addition, the serum levels of adipocytokines, including fibroblast growth factor 21 (FGF21) and adiponectin (APN), were measured.

Results Long-term HSD disrupted the growth performance of mice. Compared to those fed a normal salt diet, mice on a long-term HSD showed slower weight gain, as well as lower fat accumulation and serum levels of APN, while experiencing elevated blood pressure and levels of serum FGF21 and glucose. The 16S rRNA sequencing revealed changes in community richness and diversity, with long-term HSD affecting the abundance of certain gut microbiota, including *Firmicutes*, *Christensenella*, *Barnesiella*, and *Lactococcus*. Fecal metabolomic analysis also uncovered alterations in metabolites, such as myriocin, cerulenin, norcholic acid, 7-ketocholesterol, and prostaglandins B2. Further analysis indicated that these gut and microbiota and metabolites are predominantly involved in the lipid metabolism of the organism. Importantly, variations in these gut metabolites and microbiota were significantly correlated with body weight, fat accumulation, and the levels of FGF21 and APN.

Conclusion Long-term HSD affects physiological traits, alters gut metabolites profiles, and impacts the composition and function of gut microbiota, thus causes a certain impact on lipid metabolism.

Keywords Long-term high salt diet, Gut microbiota, Fecal metabolomics, Lipid metabolism

[†]Huiying Tian and Xiaotang Gao contributed equally to this work.

*Correspondence:

Zhuofeng Lin
zhuofenglin@wmu.edu.cn

Xianen Huang
huangxianen@wmu.edu.cn

¹ The Laboratory of Animal Center, Wenzhou Medical University, Wenzhou 325035, China

² School of Pharmaceutical Sciences, Wenzhou Medical University, Wenzhou 325035, China

³ Department of Endocrinology, The 3rd Affiliated Hospital of Wenzhou Medical University, Wenzhou 325200, China

⁴ Wenzhou Key Laboratory for the Diagnosis and Prevention of Diabetic Complication, Wenzhou 325200, China



Introduction

Sodium is an essential nutrient that plays a vital role in maintaining normal cellular homeostasis and regulating fluid and electrolyte balance. It is equally crucial for maintaining extracellular fluid volume, muscle and nerve cell function, and the transmembrane transport of nutrients and substrates, attributed to its osmotic action [1]. While the daily minimum intake level required for physiological needs remains not well established, sodium deficiency is extremely unlikely in healthy individuals due to the presence of dietary salt in commonly consumed foods [1]. Conversely, an excess of salt intake, more than physiologically necessary, is common in most populations worldwide.

Salt intake is an important worldwide public health issue [2]. The World Health Organization (WHO) recommends that the daily maximum intake of salt should not exceed 5 g in adults and should be adjusted downward for children. Data from a global 2010 study showed that the average daily intake of salt per person in the surveyed regions was 10.06 g [3]. Salt intake in Asia is among the highest in the world (14.01 g/d per capita), more than twice the recommended limit. Excessive intake of salt can lead to acute toxicity, with the possibility of a fatal outcome [1]. Chronic excessive salt intake can also lead to pathological changes in the body, although they may not be evident in the early stages. Evidence suggests that salt consumption could predict the future development of metabolic syndrome [4], which, in turn, can serve as the foundation for various metabolism disorders including insulin resistance, abnormal lipid metabolism, and elevated blood pressure [5, 6], contributing to the onset of diseases such as diabetes, non-alcoholic fatty liver disease, hypertension.

Gut microbiota is considered a bridge between diet and host health [7]. The intestinal flora and their metabolites can directly impact physiological metabolism [8]. Although salt is primarily absorbed in the upper intestine, a part of it reaches the colon [1] and interacts with the gut microbiota. Previous studies have reported the relationships between high salt consumption, gut microbiota, and body metabolism [9, 10]. However, a relatively short feeding duration may not fully reveal the long-term effects of a high salt diet (HSD).

In the present study, we established a model fed with a long-term HSD and conducted exploratory investigations into the effects of this HSD on growth performance, serum adipocytokines, and fecal microbiota composition and metabolites.

Materials and methods

Animals and treatment

All animal experiments were conducted in accordance with the Animal Research Ethics Committee of Wenzhou Medical University (Ethical approval number: SYXK 2020–0014). Seven-week-old male C57BL/6 J wild-type mice were purchased from Vital River Laboratory Animal Technology Co., Ltd. (Beijing, China) and housed in a room with free access to water and diet, at a controlled temperature of 23 ± 1 °C, and subjected to a 12-h/day light cycle. After 7 days of acclimatization, all the 8-week-old male mice were randomly divided into two groups: a high salt diet (HSD) group fed an 8% NaCl diet and a normal salt diet (NSD) group fed a 0.6% NaCl diet, for 22 weeks, with $n = 4$ in each group (cage). The HSD containing 8% NaCl was purchased from Dytes Co., Ltd. (Suzhou, China) and the NSD containing 0.6% NaCl was purchased from Cyagen Co., Ltd. (Guangzhou, China).

Sample collection and index determination

During the feeding period, the body weight of the mice was recorded every two weeks, and blood pressure was measured using tail-cuff systems (BP 2000, Visitech Systems, USA) at the start and the end of the experiment. Glucose tolerance test (GTT) was performed at the end of the experiment and glucose levels were detected and recorded from blood sample collected at 10, 20, 30, 45, 60, 75 and 90 min after glucose injection (0.01 mL/g administration). The blood glucose (BG) meter and BG test strips were purchased from Braun Co., Ltd. (Melsungen, Germany). The area under the curve (AUC) of GTT was calculated according to the formula: $AUC = 0.5 \times (BG_0 \text{ min} + BG_{30} \text{ min})/2 + 0.5 \times (BG_{30} \text{ min} + BG_{60} \text{ min})/2 + 1 \times (BG_{60} \text{ min} + BG_{90} \text{ min})/2$. On the day of sacrifice, the blood sample was collected from the eyes of the mice under anesthesia (with sodium pentobarbital at 0.1 mL/10 g body weight), blood samples were centrifuged at 3000 rpm, at 4 °C, for 10 min. The supernatant was collected and stored at -80 °C. The heart, liver, kidney, and various adipose tissues (white, peri-renal, and brown) of the mice were weighed. The intestinal feces were collected under sterile conditions, and all tissues were stored at -80 °C after cataloging. The ELISA kits for the determination of serum fibroblast growth factor 21 (FGF21) and adiponectin (APN) were purchased from Antibody and Immunoassay Service Co., Ltd. (Hong Kong, China).

Fecal metabonomics

The lyophilized feces samples were sent to Sangon Biotech (Shanghai) Co., Ltd (Shanghai, China) for metabonomics analysis. In brief, untargeted

ultrahigh-performance liquid chromatography-mass spectrometry was performed using an AB Sciex Triple TOF 5600 mass spectrometer (Waters, UK) combined with ACQUITY UPLC H-Class system (Waters, UK). Extracted samples were injected into a chromatographic column (100 mm × 2.1 mm, 1.7 μm, ACQUITY UPLC BEH C-18, Waters, UK) at a flow rate of 0.4 mL/min, an injection volume of 5 μL, and a column temperature of 45 °C. The Mobile phase consisted of phase A (water with 0.1% formic acid) and phase B (methanol with 0.1% formic acid). The elution program was as follows: 0–2 min, 5% mobile phase B; 2–4 min, 20% mobile phase B; 4–9 min, 25% mobile phase B; 9–17 min, 60% mobile phase B; 17–19 min, 100% mobile phase B; 19–20.1 min, 5% mobile phase B for equilibration. Mass spectrometry data were acquired by scanning in both positive and negative ion modes using an MS system equipped with an electrospray ionization source.

The mass spectrometry raw data were acquired using the UNIFI Scientific Information System (Ver. 1.8.1.) and processed with Progenesis QI software (Ver. 2.3, Nonlinear Dynamics, Newcastle, UK). The analytical parameters set were a precursor tolerance of 5 ppm, product tolerance of 10 ppm, and a product ion threshold of 5%. The raw abundance of metabolites was normalized as relative abundance for subsequent analysis. Metabolites annotation was performed using the Lipid metabolites and pathways strategy (Ver. 2.3) (<http://www.lipidmaps.org>), Human Metabolome Database (<https://hmdb.ca/>), and Metabolite Link database (<https://metlin.scripps.edu>).

To identify potential differential metabolites, multivariable analysis was applied for metabolite profiling. The orthogonal partial least square discriminant analysis (OPLS-DA) was implemented using “ropls” R package [11] (Ver. 1.32.0). Variable importance in the projection (VIP) was used to evaluate the importance of each metabolite in OPLS-DA model. The *p*-values from the Student’s *t*-test and VIP values were used to screen differential metabolites. Metabolite with a *p*-value < 0.05, $|\log_2(\text{Fold Change})| > 1$, and the value of VIP > 1 was considered a differential metabolite and was extracted for further analysis. KEGG pathway enrichment analysis of differential metabolites was conducted using MetaboAnalyst software (Ver. 5.0) (<https://www.metaboanalyst.ca/MetaboAnalyst/home.xhtml>).

16S rRNA gene sequencing and data analysis

The lyophilized feces samples were sent to Sangon Biotech (Shanghai) Co., Ltd (Shanghai, China) for 16S rRNA gene sequencing. Briefly, total genomic DNA was extracted, and the V3 and V4 regions of bacterial 16S rRNA gene were amplified using dual-indexed primers: 341 F: (5′-CCTACGGGNGGCWGCAG-3′) and 805R:

(5′-GACTACHVGGGTATCTAATCC-3′). The quality-qualified library was used for high-throughput sequencing on the Illumina HiSeq 2500 system (Illumina, San Diego, USA). Raw data generated from the Illumina platform were merged into sequences using PEAR [12] software (Ver. 0.9.6) based on the overlapping relationship of paired-end reads. These sequences were then divided into individual samples based on their barcode sequences. Subsequently, the data from each sample were processed to remove low-quality data and retain high-quality data using QIIME [13] software (Ver. 1.8.0). Non-specific amplification and Chimeras were also eliminated using Usearch [14] software (Ver. 5.2.236), and sequences with 97% similarity were clustered into one operational taxonomic unit (OTU). The representative sequences of each OTU were classified into different taxonomic levels (phylum, class, order, family, and genus) using the Ribosomal Database Project (RDP) classifier [15] (Ver. 2.12) with a threshold of 0.8. Additionally, the relative abundance of species was quantified at each taxonomic level.

Alpha diversity was evaluated by calculating Shannon, Simpson, Ace, and Chao1 indices with “vegan” R package (<https://github.com/vegandevs/vegan>) (Ver. 2.6–4). Using Bray–Curtis distance, principal coordinates analysis (PCoA) and non-metric multidimensional scaling (NMDS) analysis were performed to assess beta diversity. Species differences between groups were identified using Linear discriminate analysis effect size (LEfSe) based on “microeco” R package [16] (Ver. 1.1.0). The KEGG functional profiles of the microbial community were predicted by using PICRUSt2 [17] tool.

Statistical analysis

A double-blind experimental analysis mode was used, and all statistical analyses were performed using R software (Ver. 4.3.1). The normality of data distribution was assessed with the Shapiro–Wilk test. Groups comparisons were performed using either Student’s *t*-test or the Wilcoxon test. Correlation analysis of intestinal microbes, fecal metabolites, and altered indicator were estimated by Pearson correlation. The results of the statistical analysis were presented as the mean ± standard error of the mean (SEM). A level of *p*-value < 0.05 (two-sided) was considered statistically significant.

Results

Long-term HSD altered fat accumulation, glucose homeostasis, and levels of FGF21 and APN

During the feeding period, the body weight of mice fed with NSD increased gradually, while mice fed with HSD experienced a lower weight gain that did not differ significantly from their initial weight until the end of the treatment (Fig. 1 A). Moreover, the body weight of HSD-fed

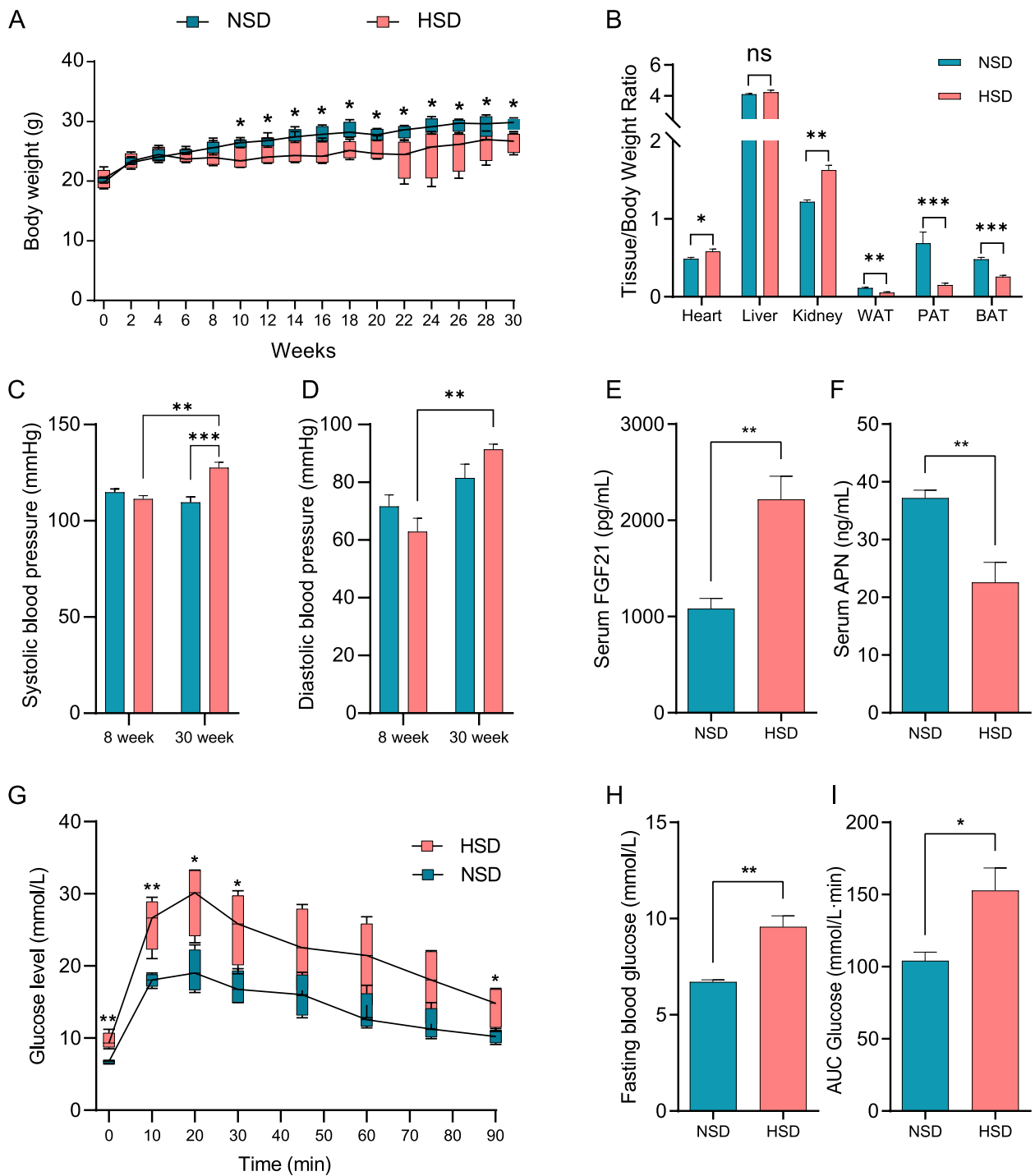


Fig. 1 Altered indicators of mice fed with long-term HSD. **A** Body weight of mice. All the 8-week-old mice were fed with NSD or HSD for 22 weeks. * $p < 0.05$ vs NSD. **B** Tissue weight to body weight ratio of mice at 30 weeks. Systolic (**C**) and diastolic (**D**) blood pressure of mice at the initiation (8 weeks) and end (30 weeks). Serum level of FGF21 (**E**) and APN (**F**) of mice at 30 weeks. **G** Glucose level of mice after injection of glucose. **H** Fasting blood glucose level of mice at 30 weeks. **I** AUC value of GTT. * $p < 0.05$ vs NSD; ** $p < 0.01$ vs NSD; *** $p < 0.001$ vs NSD; ns: no significance

mice was lower than that of NSD-fed mice at each stage. Organ and tissue weights also changed after long-term HSD treatment. The heart and kidney weight-to-body

weight ratio was elevated in long-term HSD group, while the weights of white, peri-renal, and brown adipose tissue relative to body weight decreased (Fig. 1B). In the terms

of blood pressure, both systolic and diastolic blood pressure underwent a significant elevation after long-term HSD treatment compared with the initial blood pressure (Fig. 1C, D). At the end of the treatment, systolic blood pressure was higher in long-term HSD group than that in NSD group, but diastolic blood pressure did not significantly differ between the groups. Additionally, several metabolic indicators underwent significant changes. The serum level of adipocytokines FGF21 increased in response to long-term HSD treatment, while the level of APN decreased dramatically (Fig. 1E, F). The glucose level and AUC value of GTT were higher in long-term HSD mice than in NSD group (Fig. 1G, H and I). To sum up, long-term HSD alters growth performance and metabolism homeostasis.

Overview of gut microbial communities in response to long-term HSD

The impact of intestinal microbiota on obesity and metabolic disease is widely documented [18–20]. Thus, we explored the changes in gut microbial communities in response to long-term HSD. In the present study, we acquired 749783 high-quality reads, from which 2357 representative OTUs were identified at a similarity level of 97%. The Shannon curve was plateaued with an increase in the sequences count, indicating adequate sequencing depth (Fig. 2A). Alpha diversity was assessed using several indices. The Shannon and Simpson indices in HSD group were greater compared to those in NSD group, whereas the ACE and Chao1 indices showed the opposite trend (Fig. 2B, C, D and E), indicating that gut microbial community richness and diversity were altered in response to long-term HSD. Considering species composition and abundance, we performed PCoA and NMDS analyses to assess beta diversity at the OTU level. As shown in Fig. 2F and G, long-term HSD and NSD groups were divided into two compartments in the 3D PCoA plot, and a similar pattern was observed in the NMDS score plot. Adonis ($R^2 = 0.644$, $p = 0.029$) and ANOSIM ($R^2 = 0.865$, $p = 0.028$) analyses further confirmed the significant differences between the groups.

Species annotation information for representative OTUs was identified using the RDP classifier. At the phylum level, *Firmicutes* emerged as the most predominant phylum, constituting 65.99% and 94.10% of OTUs in long-term HSD and NSD groups, respectively (Fig. 3A). The ratio of *Firmicutes* to *Bacteroidetes* was decreased in long-term HSD group (Fig. 3B). Moreover, *Bacteroidetes*, *Proteobacteria*, *Candidatus Saccharibacteria*, *Tenericutes*, and *Deferribacteres* were more enriched in long-term HSD group compared to NSD group. At the genus level, among the total 257 annotated genera, *Allobaculum* was the most abundant, representing 39.34%

and 82.19% of OTUs in long-term HSD and NSD groups, respectively (Fig. 3C). LEfSe analysis, with a threshold of an LDA score greater than 2, revealed six bacterial taxa at the phylum level showing differential abundance (Fig. 3D). The long-term HSD group exhibited a lower abundance of *Firmicutes* compared to NSD group. Conversely, the abundance of *Bacteroidetes*, *Proteobacteria*, *Candidatus-Saccharibacteria*, *Tenericutes*, and *Deferribacteres* was higher in long-term HSD (Fig. 3E). At the genus level, fifty-one bacteria showed differences in abundance, with the majority showing higher abundance in long-term HSD group, including *Barnesiella*, *Christensenella*, and *Lactococcus* (Fig. 3F). In contrast, the abundance of *Allobaculum*, *Lactobacillus*, and *Bifidobacterium* was higher in NSD group. Functional profiles extrapolation using PICRUSt2 analysis indicated significant difference in metabolism-related pathways between the groups (Fig. 4). Xenobiotics biodegradation and metabolism, lipid metabolism, metabolism of cofactors and vitamins, and glycan biosynthesis and metabolism pathways were enriched in long-term HSD group, whereas nucleotide metabolism, carbohydrate metabolism, and metabolism of terpenoids and polyketides pathways were more prevalent in NSD group.

Fecal metabolic profiling analysis of high salt intake

In view of the potential disturbance in metabolic balance caused by long-term HSD, further analysis was conducted in fecal metabolism profiling. The overall PCA plot of all samples, shown in Fig. 5A, demonstrated that all samples were divided into two clusters, and long-term HSD and NSD groups were clustered in distinct areas of PCA plot, indicating limited variation within per group and high differences between the groups. The R2 and Q2 values serve as the parameters for evaluating the interpretative and predictive abilities of OPLS-DA model, respectively. In the present study, R2X (cum) = 0.442, R2Y (cum) = 0.999, and Q2 = 0.874, suggesting that the OPLS-DA model exhibited excellent robustness and predictive ability.

Based on untargeted ultrahigh-performance liquid chromatography–mass spectrometry, a total of 4686 metabolites were annotated. Fatty acyls, constituting 15.56% of the metabolites, were the most prominent, followed by glycerophospholipids at 13.06% (Fig. 5B). According to the criteria ($VIP > 1$, $|\log_2(\text{Fold Change})| > 1$ and $p < 0.05$), 644 differential metabolites were identified, with 326 metabolites up-regulated and 318 down-regulated in long-term HSD group (Fig. 5C). Lipids, including fatty acyls, glycerophospholipids, prenol lipids, steroids lipids, and steroids and steroid derivatives, were the predominant differential metabolites, comprising over half of the differential metabolites quantities (Fig. 5D).

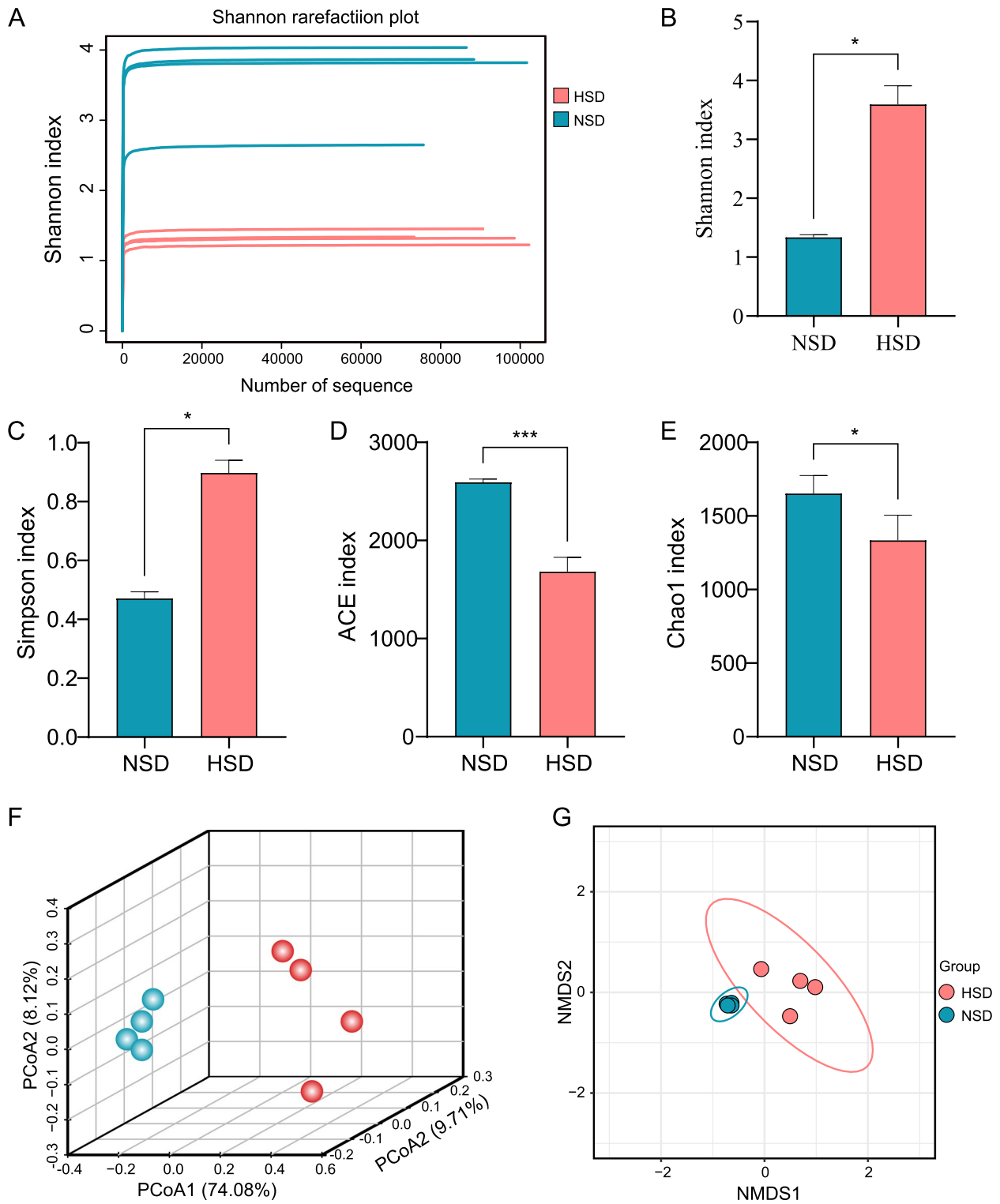


Fig. 2 Alpha and beta diversity analysis. **A** Shannon rarefaction plot. Shannon (**B**), Simpson (**C**), ACE (**D**), and Chao1 (**E**) indices. **F** 3D plot of PCoA. **G** NMDs analysis. * $p < 0.05$ vs NSD; *** $p < 0.001$ vs NSD Firmicutes/Bacteroidetes ratio

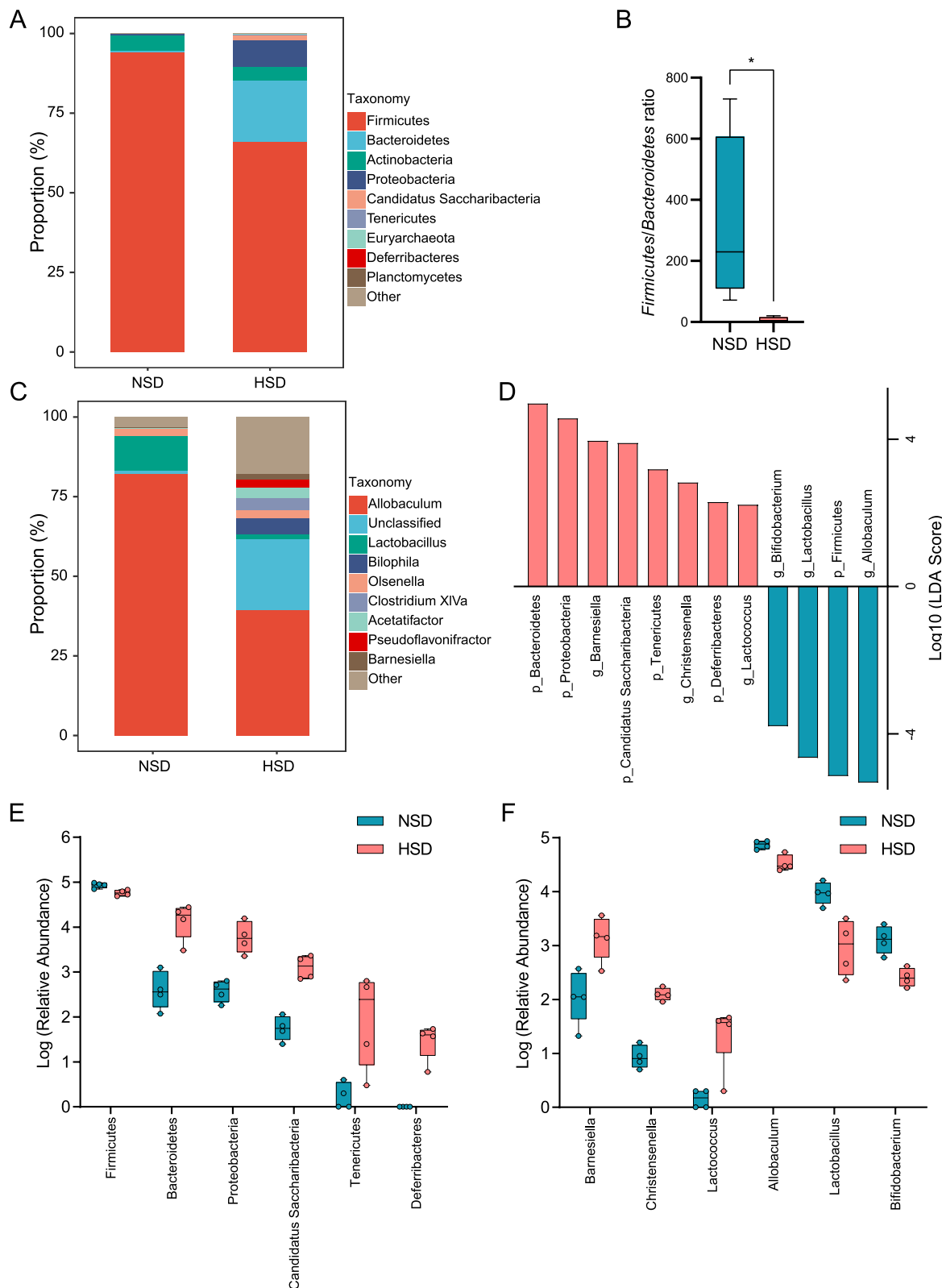


Fig. 3 Differential analysis of gut microbial community. **A** Taxonomic proportion of gut microbiota at phylum. **B** the ratio of Firmicutes to Bacteroidetes. **C** Taxonomic proportion of gut microbiota at genus. **D** Histogram of LDA value distribution. Relative abundance of differential microbiotas at phylum (**E**) and genus (**F**). * $p < 0.05$ vs NSD

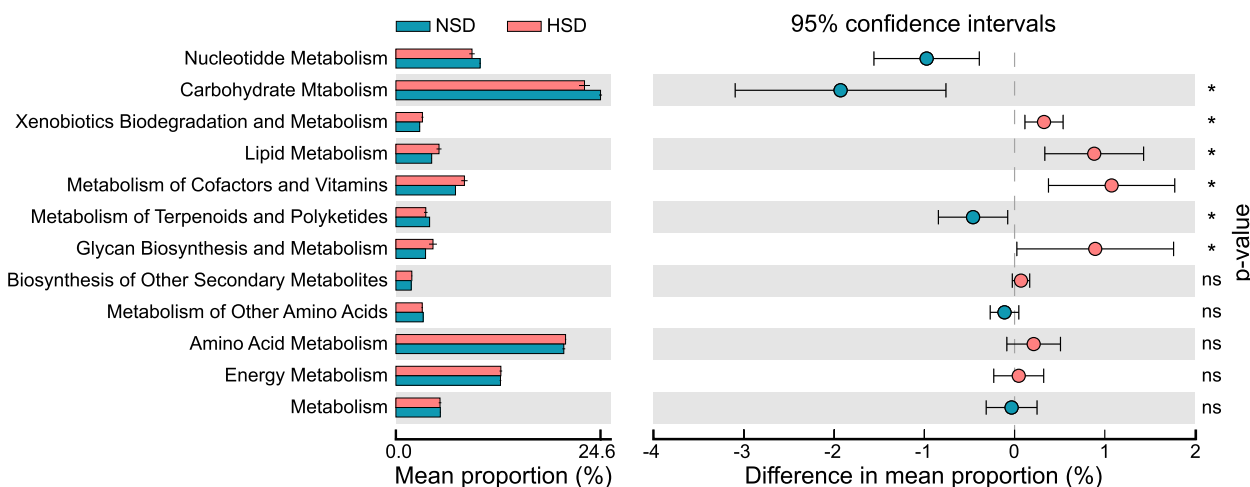


Fig. 4 STAMP plot shows the differential pathways. * $p < 0.05$ vs NSD; ns: no significance

In comparison to NSD group, myriocin, norcholeic acid, cerulenin, and 7-ketocholesterol levels increased, while prostaglandin B2 decreased in long-term HSD group (Fig. 5E). Further pathway enrichment analysis revealed that three lipid metabolism-related pathways (linoleic acid metabolism, steroid hormone biosynthesis, and steroid biosynthesis) were significantly enriched in long-term HSD group (Fig. 5F), suggesting that long-term HSD disrupts lipid metabolism balance.

Correlation analysis of intestinal microbes, fecal metabolites, and altered indicator

The relationships between intestinal microbes, fecal metabolites, and altered indicators were assessed through correlation analysis to investigate key gut microbes and fecal metabolites responsible for changes induced by long-term high salt intake (Fig. 6). Specifically, *Christensenella* displayed a negative correlation with WAT ($r = -0.805$) and APN ($r = -0.812$), but a positive correlation with FGF21 ($r = 0.831$). Conversely, *Firmicutes* showed a positive correlation with body weight ($r = 0.744$) and a negative correlation with FGF21 ($r = -0.942$). In contrast, *Barnesiella* exhibited a negative correlation with body weight ($r = -0.750$) and a positive correlation with FGF21 ($r = 0.773$). *Lactococcus* was found to be negatively correlated with both WAT ($r = -0.806$) and APN ($r = -0.833$). Furthermore, several metabolites showed notable correlations: Myriocin, 7-ketocholesterol, norcholeic acid, and cerulenin were negatively correlated with body weight ($r = -0.723$ for myriocin, $r = -0.877$ for 7-ketocholesterol, $r = -0.849$ for cerulenin), and WAT ($r = -0.660$ for myriocin), as well as APN ($r = -0.794$ for myriocin, $r = -0.732$ for 7-ketocholesterol, $r = -0.726$ for norcholeic acid), but positively

correlated with FGF21 ($r = 0.944$ for myriocin, $r = 0.762$ for 7-ketocholesterol, $r = 0.983$ for norcholeic acid, $r = 0.798$ for cerulenin). Additionally, prostaglandin B2 was positively correlated with WAT ($r = 0.708$), and negatively correlated with FGF21 ($r = -0.899$).

Discussion

Dietary salt is an essential micronutrient for maintaining life activity. High salt consumption, however, has been linked to adverse outcomes, including exacerbation of metabolism function and contribution to metabolic syndrome [21, 22]. The long-term effects of high salt intake on organisms are not well-documented. In the present study, we developed a mouse model to explore the changes in organisms responsible for long-term HSD. We observed that long-term HSD impacted growth, metabolism homeostasis, and altered gut microbiota and metabolites profiling. Interestingly, mice fed with long-term HSD experienced lower weight gain and fat accumulation, which is opposite to previous results that high salt leads to obesity [23, 24]. One reasonable explanation for this discrepancy is that high salt intake causes hyperphagia in mice, yet body weight remains stable under ad libitum dietary conditions due to a hypercatabolic state [25]. Our observation of stable body weight and reduced WAT in long-term HSD group after consuming high salt lend support to this hypothesis.

Further investigation into the mechanisms revealed increased gut microbial diversity with long-term HSD, consistent with previous findings of decreased microbial diversity in obesity [26]. Notably, the abundance of *Firmicutes* and *Bacteroidetes* seems to be related to fat metabolism. The ratio of *Firmicutes*/*Bacteroidetes* is linked to obesity and metabolic disorders [27], and is

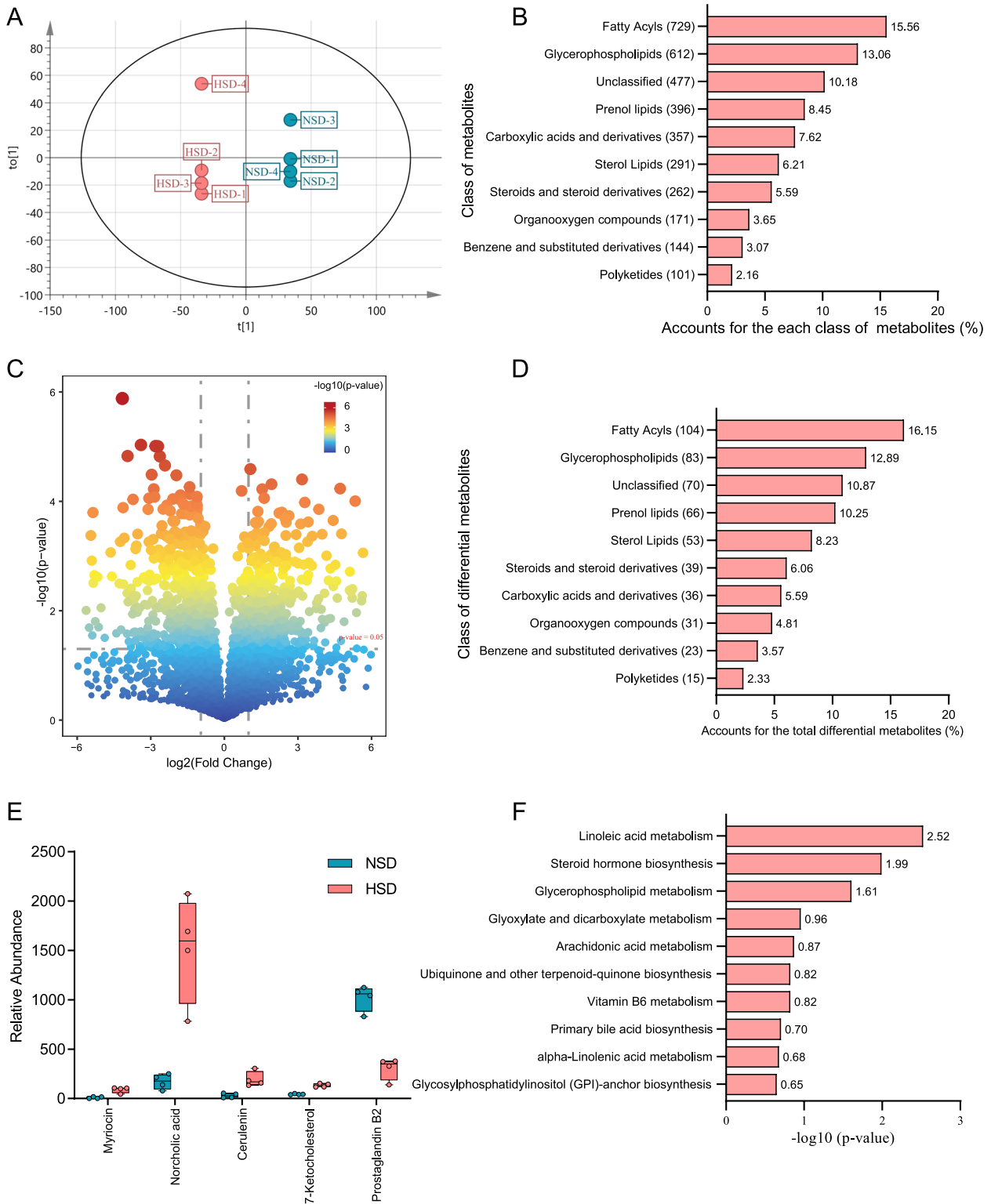


Fig. 5 Fecal metabolomics analysis. **A** OPLS-DA analysis. **B** Top 10 class of total metabolites. **C** Volcano plot of differential metabolite analysis. **D** Top 10 class of differential metabolites. **E** Relative abundance of differential metabolites. **F** Pathway analysis showed that differential metabolites were enriched pathways, including linoleic acid metabolism, steroid hormone biosynthesis, and steroid biosynthesis. The rest are the involved pathways without significant differences

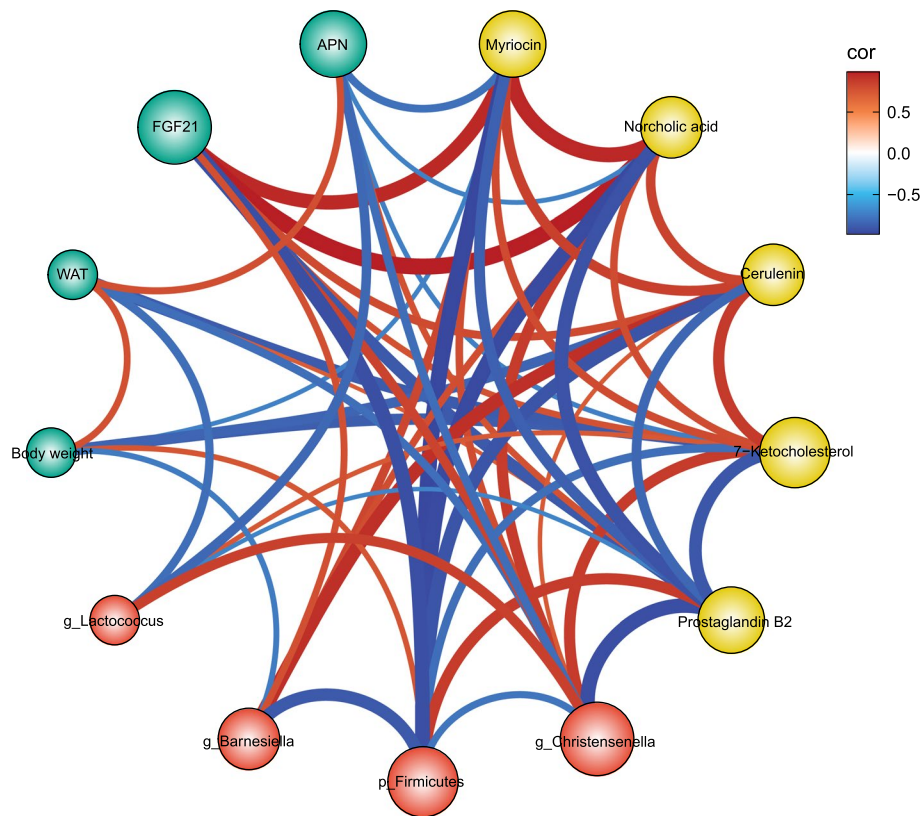


Fig. 6 Correlation analysis among gut microbiota, metabolite, and body weight, WAT, FGF21, and APN. Red and blue refer to significant positive and negative correlation, respectively. All $p < 0.05$; $p > 0.05$ no showed

considered as a vital index to measuring obesity [28, 29]. Recent studies have indicated that individuals with obesity exhibited a higher relative abundance of Firmicutes and a lower relative abundance of Bacteroidetes [29, 30]. Additionally, a reduction of *Firmicutes/Bacteroidetes* ratio showed a promising prospect for anti-obesity effect [31, 32]. In our study, consumption of high salt altered the abundance of *Bacteroidetes* and *Firmicutes* and *Firmicutes/Bacteroidetes* ratio. Furthermore, the changes in abundance of *Firmicutes* were positively correlated with changes in body weight. These findings suggested that reduced abundance of *Firmicutes* may, at least partially, explain the changes in body weight. At the genus level, long-term high salt consumption decreased the abundance of *Allobaculum*, *Lactobacillus*, and *Bifidobacterium*, which was broadly in line with previous studies [22, 33]. Moreover, long-term high salt intake increased the abundance of *Barnesiella*, *Christensenella*, and *Lactococcus*, which were rarely reported to be associated with HSD. *Barnesiella* significantly correlated with hepatic lipid accumulation [34]. *Christensenella* had a high correlation with obesity and obesity-related metabolic disorders of the host [35]. Conversely, *Lactococcus* abundance had a negative correlation with obesity [36] and an

alleviating effect on diet-induced obesity, fat accumulation, and adipose tissue metabolism [37].

It is widely demonstrated that dietary structure could affect the gut microbiome composition, which is accompanied by the alternation of intestinal metabolites, thereby contributing to several metabolic disorders. Similar to the results of intestinal microbes, long-term HSD also provoked significant changes in fecal metabolites, particularly lipid metabolites. Specifically, the levels of myriocin, cerulenin, norcholic acid, and 7-ketocholesterol were significantly increased, while the level of prostaglandins B2 was decreased after fed with long-term high salt. Myriocin has been shown to possess beneficial effects on attenuating body weight and lipid accumulation, as well as regulating fatty acid metabolism [38, 39]. Moreover, myriocin inhibited the synthesis of ceramide [39] which was reported to stimulate lipid uptake and storage [40]. Similarly, cerulenin plays an important role in promoting weight loss and steatosis by blocking fatty acid synthase [41]. Norcholic acid is involved in bile acid metabolism and may serve as a key regulator for improving hyperlipidemia [42]. 7-ketocholesterol has been seen as a novel adipokine modulating the adipogenic potential of undifferentiated adipose precursor cells [43], and

showed the abilities accelerating hepatic lipid accumulation and downregulating fatty acid oxidation [44]. Despite the link between prostaglandins E and obesity and lipolysis being widely documented [28, 45–47], there was little focus on prostaglandins B2. Further pathway enrichment analysis results that three lipid metabolism-related pathways were significantly enriched in HSD group supported a viewpoint that lipid metabolism was disturbed by long-term high salt, which is partially evidenced by previous studies [48].

We also identified several potential interaction relationships between gut bacteria or metabolites and FGF21 and APN. The results indicated that *Christensenella*, *Firmicutes*, *Barnesiella*, *Lactococcus*, myriocin, cerulenin, norcholic acid, 7-ketocholesterol, and prostaglandins B2 were positively or negatively correlated with FGF21 or APN. Previous research has reported that *Lactococcus* could prevent the proliferation of adipogenic transcription factors APN and effectively alleviates diet-induced obesity and lipid deposition [37]. Moreover, myriocin is involved in lipid metabolism, which could reduce fat deposition by inhibiting the synthesis of ceramide [39]. Similarly, FGF21 could regulate the secretion of APN, and inhibit the level of ceramide, then form an FGF21-APN-ceramide axis to control energy metabolism and insulin action [49]. Consequently, these interactions may provide a novel insight into understanding the complicated regulatory network of gut bacteria, fecal metabolites, and FGF21 or APN.

Nonetheless, our research is not without limitations. Firstly, this is a preliminary exploration study, the sample size for the sequencing analysis research is small. Insufficient sample size will lead to unreliable conclusions, large errors, insufficient statistical significance, and overfitting of the model, so the reliability and practical application value of the data analysis results are limited. Secondly, how the altered microbial communities and metabolites performed a function for lipid metabolism remain fully ambiguous, using germ-free mice to confirm the bacteria to be interested will be needed. Thirdly, the time dependent changes in the microbiome during this high salt intervention and the the metabolite's levels in serum will be much more relevant considering the impact of the long treatment to the host metabolism. Thus, further studies are needed to validate our results.

Conclusion

In summary, our research revealed that long-term HSD stimulates FGF21 secretion in mice, alongside diminishing weight gain, white fat accumulation, and level of APN.

Integrated 16S rRNA sequencing and fecal metabolomic analysis showed that long-term HSD impacts gut

microbiota and metabolites profiles, including *Firmicutes*, *Christensenella*, *Barnesiella*, and *Lactococcus*, as well as myriocin, cerulenin, norcholic acid, 7-ketocholesterol, and prostaglandins B2. These gut bacteria and metabolites were significantly correlated with decreased body weight and white fat accumulation, and altered levels of FGF21 and APN, and potentially play a crucial role in lipid metabolism of organism.

Abbreviations

HSD	High Salt Diet
FGF21	Fibroblast Growth Factor 21
APN	Adiponectin
WHO	World Health Organization
GTT	Glucose Tolerance Test
BG	Blood Glucose
AUC	Area Under the Curve
NSD	Normal Salt Diet
OPLS-DA	The Orthogonal Partial Least Square Discriminant Analysis
KEGG	Kyoto Encyclopedia of Genes and Genomes
OTU	Operational Taxonomic unit
RDP	Ribosomal Database Project
PCoA	Principal Coordinates Analysis
NMDS	Non-Metric Multidimensional Scaling

Acknowledgements

We thank Dr. Jing Gan, and Dr. Yuanrong Chen for their technical support related to the statistical analysis of data and revising our manuscript.

Authors' contributions

H.T., and X.G. performed the experiments, analyzed the data, and drafted the manuscript. H.D. supported executing in vivo experiments and data analysis. X.H., and Z.L. developed the concept, designed the study, and revised the manuscript. All authors have read, discussed the results, and approved the manuscript.

Funding

This research was supported by China National Funds for Distinguished Young Scientists (81925004).

Data availability

All data generated or analysed during this study are reasonably available from the corresponding author. The raw data of 16S rRNA sequencing data generated in this study were deposited to NCBI Sequence Read Archive (SRA) under accession number SRP501153.

Declarations

Ethics approval and consent to participate

The written consent was obtained from the Animal Research Ethics Committee of Wenzhou Medical University, and the protocol was approved by the Animal Research Ethics Committee of Wenzhou Medical University, with approval number SYXK 2020–0014.

Consent for publication

Not applicable.

Competing interests

The authors declare no competing interests.

Received: 2 July 2024 Accepted: 4 March 2025
Published online: 15 May 2025

References

- Strazzullo P, Leclercq C. Sodium. *Adv Nutr*. 2014;5(2):188–90. <https://doi.org/10.3945/an.113.005215>.
- Brown IJ, Tzoulaki I, Candeiias V, Elliott P. Salt intakes around the world: implications for public health. *Int J Epidemiol*. 2009;38(3):791–813. <https://doi.org/10.1093/ije/dyp139>.
- Powles J, Fahimi S, Micha R, Khatibzadeh S, Shi P, Ezzati M, Engell RE, Lim SS, Danaei G, Mozaffarian D. Global, regional and national sodium intakes in 1990 and 2010: a systematic analysis of 24 h urinary sodium excretion and dietary surveys worldwide. *BMJ Open*. 2013;3(12):e003733. <https://doi.org/10.1136/bmjopen-2013-003733>.
- Takase H, Hayashi K, Kin F, Nakano S, Machii M, Takayama S, Sugiura T, Dohi Y. Dietary salt intake predicts future development of metabolic syndrome in the general population. *Hypertens Res*. 2023;46(1):236–43. <https://doi.org/10.1038/s41440-022-01035-7>.
- Xu J, Mao F. Role of high-salt diet in non-alcoholic fatty liver disease: a mini-review of the evidence. *Eur J Clin Nutr*. 2022;76(8):1053–9. <https://doi.org/10.1038/s41430-021-01044-8>.
- Pearson JT, Thambyah HP, Waddingham MT, Inagaki T, Sukumaran V, Ngo JP, Ow CPC, Sonobe T, Chen YJ, Edgley AJ, Fujii Y, Du CK, Zhan DY, Umetani K, Kelly DJ, Tsuchimochi H, Shirai M. β -blockade prevents coronary macro- and microvascular dysfunction induced by a high salt diet and insulin resistance in the Goto-Kakizaki rat. *Clin Sci (Lond)*. 2021;135(2):327–46. <https://doi.org/10.1042/cs20201441>.
- Zhao J, Zhang X, Liu H, Brown MA, Qiao S. Dietary protein and gut microbiota composition and function. *Curr Protein Pept Sci*. 2019;20(2):145–54. <https://doi.org/10.2174/1389203719666180514145437>.
- O'Connor EM. The role of gut microbiota in nutritional status. *Curr Opin Clin Nutr Metab Care*. 2013;16(5):509–16. <https://doi.org/10.1097/MCO.0b013e3283638eb3>.
- Wang C, Huang Z, Yu K, Ding R, Ye K, Dai C, Xu X, Zhou G, Li C. High-salt diet has a certain impact on protein digestion and gut microbiota: a sequencing and proteome combined study. *Front Microbiol*. 2017;8:1838. <https://doi.org/10.3389/fmicb.2017.01838>.
- Chen X, Zhang Z, Cui B, Jiang A, Tao H, Cheng S, Liu Y. Combination of chronic alcohol consumption and high-salt intake elicits gut microbial alterations and liver steatosis in mice. *J Agric Food Chem*. 2020;68(6):1750–9. <https://doi.org/10.1021/acs.jafc.9b07368>.
- Thévenot EA, Roux A, Xu Y, Ezan E, Junot C. Analysis of the human adult urinary metabolome variations with age, body mass index, and gender by implementing a comprehensive workflow for univariate and OPLS statistical analyses. *J Proteome Res*. 2015;14(8):3322–35. <https://doi.org/10.1021/acs.jproteome.5b00354>.
- Zhang J, Kobert K, Flouri T, Stamatakis A. PEAR: a fast and accurate Illumina Paired-End reAd mergeR. *Bioinformatics*. 2014;30(5):614–20. <https://doi.org/10.1093/bioinformatics/btt593>.
- Caporaso JG, Kuczynski J, Stombaugh J, Bittinger K, Bushman FD, Costello EK, Fierer N, Peña AG, Goodrich JK, Gordon JJ, Huttley GA, Kelley ST, Knights D, Koenig JE, Ley RE, Lozupone CA, McDonald D, Muegge BD, Pirrung M, Reeder J, Sevinsky JR, Turnbaugh PJ, Walters WA, Widmann J, Yatsunenko T, Zaneveld J, Knight R. QIIME allows analysis of high-throughput community sequencing data. *Nat Methods*. 2010;7(5):335–6. <https://doi.org/10.1038/nmeth.f.303>.
- Edgar RC. Search and clustering orders of magnitude faster than BLAST. *Bioinformatics*. 2010;26(19):2460–1. <https://doi.org/10.1093/bioinformatics/btq461>.
- Wang Q, Garrity GM, Tiedje JM, Cole JR. Naive Bayesian classifier for rapid assignment of rRNA sequences into the new bacterial taxonomy. *Appl Environ Microbiol*. 2007;73(16):5261–7. <https://doi.org/10.1128/aem.00062-07>.
- Liu C, Cui Y, Li X, Yao M. microeco: an R package for data mining in microbial community ecology. *FEMS Microbiol Ecol*. 2021;97(2):fiaa255. <https://doi.org/10.1093/femsec/fiaa255>.
- Douglas GM, Maffei VJ, Zaneveld JR, Yurgel SN, Brown JR, Taylor CM, Huttenhower C, Langille MGI. PICRUSt2 for prediction of metagenome functions. *Nat Biotechnol*. 2020;38(6):685–8. <https://doi.org/10.1038/s41587-020-0548-6>.
- Boulangé CL, Neves AL, Chilloux J, Nicholson JK, Dumas ME. Impact of the gut microbiota on inflammation, obesity, and metabolic disease. *Genome Med*. 2016;8(1):42. <https://doi.org/10.1186/s13073-016-0303-2>.
- Fan Y, Pedersen O. Gut microbiota in human metabolic health and disease. *Nat Rev Microbiol*. 2021;19(1):55–71. <https://doi.org/10.1038/s41579-020-0433-9>.
- Cani PD, Van Hul M, Lefort C, Depommier C, Rastelli M, Everard A. Microbial regulation of organismal energy homeostasis. *Nat Metab*. 2019;1(1):34–46. <https://doi.org/10.1038/s42255-018-0017-4>.
- Wu Q, Burley G, Li LC, Lin S, Shi YC. The role of dietary salt in metabolism and energy balance: Insights beyond cardiovascular disease. *Diabetes Obes Metab*. 2023;25(5):1147–61. <https://doi.org/10.1111/dom.14980>.
- Wilck N, Matus MG, Kearney SM, Olesen SW, Forslund K, Bartolomeaus H, Haase S, Mähler A, Balogh A, Markó L, Vvedenskaya O, Kleiner FH, Tsvetkov D, Klug L, Costea PI, Sunagawa S, Maier L, Rakova N, Schatz V, Neubert P, Frätzer C, Krannich A, Gollasch M, Grohme DA, Côte-Real BF, Gerlach RG, Basic M, Typas A, Wu C, Titze JM, Jantsch J, Boschmann M, Dechend R, Kleinewietfeld M, Kempa S, Bork P, Linker RA, Alm EJ, Müller DN. Salt-responsive gut commensal modulates T(H)17 axis and disease. *Nature*. 2017;551(7682):585–9. <https://doi.org/10.1038/nature24628>.
- Dobrian AD, Schriver SD, Lynch T, Prewitt RL. Effect of salt on hypertension and oxidative stress in a rat model of diet-induced obesity. *Am J Physiol Renal Physiol*. 2003;285(4):F619–628. <https://doi.org/10.1152/ajprenal.00388.2002>.
- Lanaspa MA, Kuwabara M, Andres-Hernando A, Li N, Cicerchi C, Jensen T, Orlicky DJ, Roncal-Jimenez CA, Ishimoto T, Nakagawa T, Rodriguez-Iturbe B, MacLean PS, Johnson RJ. High salt intake causes leptin resistance and obesity in mice by stimulating endogenous fructose production and metabolism. *Proc Natl Acad Sci U S A*. 2018;115(12):3138–43. <https://doi.org/10.1073/pnas.1713837115>.
- Kitada K, Daub S, Zhang Y, Klein JD, Nakano D, Pedchenko T, Lantier L, LaRocque LM, Marton A, Neubert P, Schröder A, Rakova N, Jantsch J, Dikalova AE, Dikalov SI, Harrison DG, Müller DN, Nishiyama A, Rauh M, Harris RC, Luft FC, Wassermann DH, Sands JM, Titze J. High salt intake re-prioritizes osmolyte and energy metabolism for body fluid conservation. *J Clin Invest*. 2017;127(5):1944–59. <https://doi.org/10.1172/jci88532>.
- Cheng Z, Zhang L, Yang L, Chu H. The critical role of gut microbiota in obesity. *Front Endocrinol (Lausanne)*. 2022;13:1025706. <https://doi.org/10.3389/fendo.2022.1025706>.
- Zhu Y, Lin X, Zhao F, Shi X, Li H, Li Y, Zhu W, Xu X, Li C, Zhou G. Meat, dairy and plant proteins alter bacterial composition of rat gut bacteria. *Sci Rep*. 2015;5:15220. <https://doi.org/10.1038/srep15220>.
- Turnbaugh PJ, Ley RE, Mahowald MA, Magrini V, Mardis ER, Gordon JL. An obesity-associated gut microbiome with increased capacity for energy harvest. *Nature*. 2006;444(7122):1027–31. <https://doi.org/10.1038/nature05414>.
- Abdallah Ismail N, Ragab SH, AbdElbaky A, Shoeib AR, Alhosary Y, Fekry D. Frequency of Firmicutes and Bacteroidetes in gut microbiota in obese and normal weight Egyptian children and adults. *Arch Med Sci*. 2011;7(3):501–7. <https://doi.org/10.5114/aoms.2011.23418>.
- Zhang Y, Tang K, Deng Y, Chen R, Liang S, Xie H, He Y, Chen Y, Yang Q. Effects of shenling baizhu powder herbal formula on intestinal microbiota in high-fat diet-induced NAFLD rats. *Biomed Pharmacother*. 2018;102:1025–36. <https://doi.org/10.1016/j.biopha.2018.03.158>.
- Baek GH, Yoo KM, Kim SY, Lee DH, Chung H, Jung SC, Park SK, Kim JS. Collagen peptide exerts an anti-obesity effect by influencing the firmicutes/bacteroidetes ratio in the gut. *Nutrients*. 2023;15(11):2610. <https://doi.org/10.3390/nu15112610>.
- Turnbaugh PJ, Bäckhed F, Fulton L, Gordon JL. Diet-induced obesity is linked to marked but reversible alterations in the mouse distal gut microbiome. *Cell Host Microbe*. 2008;3(4):213–23. <https://doi.org/10.1016/j.chom.2008.02.015>.
- Hamad I, Cardilli A, Côte-Real BF, Dyczko A, Vangronsveld J, Kleinewietfeld M. High-salt diet induces depletion of lactic acid-producing bacteria in murine gut. *Nutrients*. 2022;14(6):1171. <https://doi.org/10.3390/nu14061171>.
- Rodriguez J, Hiel S, Neyrinck AM, Le Roy T, Pötgens SA, Leyrolle Q, Pachikian BD, Gianfrancesco MA, Cani PD, Paquot N, Cnop M, Lanthier N, Thissen JP, Bindels LB, Delzenne NM. Discovery of the gut microbial signature driving the efficacy of prebiotic intervention in obese patients. *Gut*. 2020;69(11):1975–87. <https://doi.org/10.1136/gutjnl-2019-319726>.
- Song Y, Shen H, Liu T, Pan B, De Alwis S, Zhang W, Luo X, Li Z, Wang N, Ma W, Zhang T. Effects of three different mannans on obesity

- and gut microbiota in high-fat diet-fed C57BL/6J mice. *Food Funct.* 2021;12(10):4606–20. <https://doi.org/10.1039/d0fo03331f>.
36. Zhang M, Liu J, Li C, Gao J, Xu C, Wu X, Xu T, Cui C, Wei H, Peng J, Zheng R. Functional fiber reduces mice obesity by regulating intestinal microbiota. *Nutrients.* 2022;14(13):2676. <https://doi.org/10.3390/nu14132676>.
37. Zhang Q, Kim JH, Kim Y, Kim W. *Lactococcus chungangensis* CAU 28 alleviates diet-induced obesity and adipose tissue metabolism in vitro and in mice fed a high-fat diet. *J Dairy Sci.* 2020;103(11):9803–14. <https://doi.org/10.3168/jds.2020-18681>.
38. Signorelli P, Pivari F, Barcella M, Merelli I, Zulueta A, Dei Cas M, Rosso L, Ghidoni R, Caretti A, Paroni R, Mingione A. Myriocin modulates the altered lipid metabolism and storage in cystic fibrosis. *Cell Signal.* 2021;81:109928. <https://doi.org/10.1016/j.cellsig.2021.109928>.
39. Yang RX, Pan Q, Liu XL, Zhou D, Xin FZ, Zhao ZH, Zhang RN, Zeng J, Qiao L, Hu CX, Xu GW, Fan JG. Therapeutic effect and autophagy regulation of myriocin in nonalcoholic steatohepatitis. *Lipids Health Dis.* 2019;18(1):179. <https://doi.org/10.1186/s12944-019-1118-0>.
40. Chaurasia B, Summers SA. Ceramides in metabolism: key lipotoxic players. *Annu Rev Physiol.* 2021;83:303–30. <https://doi.org/10.1146/annurev-physiol-031620-093815>.
41. Cheng G, Palanisamy AP, Evans ZP, Sutter AG, Jin L, Singh I, May H, Schmidt MG, Chavin KD. Cerulenin blockade of fatty acid synthase reverses hepatic steatosis in ob/ob mice. *PLoS One.* 2013;8(9):e75980. <https://doi.org/10.1371/journal.pone.0075980>.
42. Li X, Xiao Y, Huang Y, Song L, Li M, Ren Z. *Lactobacillus gasserii* RW2014 ameliorates hyperlipidemia by modulating bile acid metabolism and gut microbiota composition in rats. *Nutrients.* 2022;14(23):4945. <https://doi.org/10.3390/nu14234945>.
43. Murdolo G, Piroddi M, Tortoioli C, Bartolini D, Schmelz M, Luchetti F, Canonico B, Papa S, Zerbinati C, Iuliano L, Galli F. Free radical-derived oxysterols: novel adipokines modulating adipogenic differentiation of adipose precursor cells. *J Clin Endocrinol Metab.* 2016;101(12):4974–83. <https://doi.org/10.1210/jc.2016-2918>.
44. Chang J, Koseki M, Saga A, Kanno K, Higo T, Okuzaki D, Okada T, Inui H, Tanaka K, Asaji M, Zhu Y, Kamada Y, Ono M, Saibara T, Ichi I, Ohama T, Nishida M, Yamashita S, Sakata Y. Dietary Oxysterol, 7-Ketocholesterol Accelerates Hepatic Lipid Accumulation and Macrophage Infiltration in Obese Mice. *Front Endocrinol (Lausanne).* 2020;11:614692. <https://doi.org/10.3389/fendo.2020.614692>.
45. Curtis-Prior PB. Prostaglandins and obesity. *Lancet.* 1975;1(7912):897–9. [https://doi.org/10.1016/s0140-6736\(75\)91690-6](https://doi.org/10.1016/s0140-6736(75)91690-6).
46. Chatzipanteli K, Rudolph S, Axelrod L. Coordinate control of lipolysis by prostaglandin E2 and prostacyclin in rat adipose tissue. *Diabetes.* 1992;41(8):927–35. <https://doi.org/10.2337/diab.41.8.927>.
47. Richelsen B. Prostaglandin E2 action and binding in human adipocytes: effects of sex, age, and obesity. *Metabolism.* 1988;37(3):268–75. [https://doi.org/10.1016/0026-0495\(88\)90107-2](https://doi.org/10.1016/0026-0495(88)90107-2).
48. Yan X, Jin J, Su X, Yin X, Gao J, Wang X, Zhang S, Bu P, Wang M, Zhang Y, Wang Z, Zhang Q. Intestinal flora modulates blood pressure by regulating the synthesis of intestinal-derived corticosterone in high salt-induced hypertension. *Circ Res.* 2020;126(7):839–53. <https://doi.org/10.1161/circresaha.119.316394>.
49. Holland WL, Adams AC, Brozinick JT, Bui HH, Miyauchi Y, Kusminski CM, Bauer SM, Wade M, Singhal E, Cheng CC, Volk K, Kuo MS, Gordillo R, Kharitonov A, Scherer PE. An FGF21-adiponectin-ceramide axis controls energy expenditure and insulin action in mice. *Cell Metab.* 2013;17(5):790–7. <https://doi.org/10.1016/j.cmet.2013.03.019>.

Publisher's Note

Springer Nature remains neutral with regard to jurisdictional claims in published maps and institutional affiliations.